

Aerial Transportation of Unknown Payloads: Adaptive Path Tracking for Quadrotors

by

Viswa Narayan, Spandan Roy, Simone Baldi

in

IROS

Report No: IIIT/TR/2020/-1



Centre for Robotics
International Institute of Information Technology
Hyderabad - 500 032, INDIA
October 2020

Aerial Transportation of Unknown Payloads: Adaptive Path Tracking for Quadrotors

Viswa N. Sankaranarayanan¹, Spandan Roy¹ and Simone Baldi²

Abstract—With the advent of intelligent transport, quadrotors are becoming an attractive aerial transport solution during emergency evacuations, construction works etc. During such operations, dynamic variations in (possibly unknown) payload and unknown external disturbances cause considerable control challenges for path tracking algorithms. In fact, the state-dependent nature of the resulting uncertainties makes state-of-the-art adaptive control solutions ineffective against such uncertainties that can be *completely unknown and possibly unbounded a priori*. This paper, to the best of the knowledge of the authors, proposes the first adaptive control solution for quadrotors, which does not require any a priori knowledge of the parameters of quadrotor dynamics as well as of external disturbances. The stability of the closed-loop system is studied analytically via Lyapunov theory and the effectiveness of the proposed solution is verified on a realistic simulator.

I. INTRODUCTION

Over the past two decades, quadrotors have been a source of considerable research interest owing to its advantages such as simple structure, vertical taking off and landing, rapid maneuvering etc. [1]–[3]. Such advantages are crucial in various military and civil applications such as surveillance, fire fighting, environmental monitoring to name a few [4], [5]. Most recently, global research is more and more interested in smart transport systems, where quadrotors are used in package delivery, construction works, disaster relief operation as a mode of smart aerial transportation [6], [7].

Despite the fact that carrying payload via a suspended cable is one of the most common ways for a quadrotor [6]–[8], it may not be optimal/desirable in indoor scenarios, especially in disaster sites, where the quadrotor might need to manoeuvre through constrained altitudes. In such scenarios, rigidly attaching a payload would be a preferred mode, which also provides the flexibility to autonomously pickup and drop the payload. From a research point of view, crucial control challenges during aerial transportation arise from drastic variation in the mass and inertia of the quadrotor due to unknown payload, imprecise knowledge of the quadrotor parameters and unknown external disturbances.

This work was partly supported by Ministry of Electronics and Information Technology, MeitY, India, by the Fundamental Research Funds for the Central Universities grant no. 4007019109 (RECON-STRUCT) and by the special guiding funds “double first-class” grant no. 4007019201 and by the IIT-H seed grant no. 19-20/003.

¹V. Sankaranarayanan and S. Roy are with Robotics Research Center, International Institute of Information Technology Hyderabad (IIIT-H), Hyderabad, India (viswa.narayanan@research.iiit.ac.in, spandan.roy@iiit.ac.in)

²S. Baldi is with School of CyberScience and Engineering, Southeast University, Nanjing, China and with School of Mathematics, Southeast University, Nanjing, China (s.baldi@tudelft.nl)

In the following, we present state-of-the-art control designs for quadrotors, together with existing challenges and the contributions brought out by this research work.

A. Related Works and Contribution

To operate a quadrotor under uncertain scenarios, researchers have inevitably looked into robust control [9]–[12] and adaptive control methods [7], [13]–[20]. However, robust control methods [9]–[12] rely on precise knowledge of mass matrix; on the other hand, the adaptive control designs [7], [13]–[16], [18]–[20] require a priori knowledge of system structures and of bounds on external disturbances. Such constraints are often difficult to be satisfied in practice due to unknown payload and external disturbances.

To avoid a priori knowledge of bounds on uncertainties, researchers have recently applied adaptive sliding mode designs [17], [21]–[23] considering uncertainties to be a priori bounded. However, when such assumption is not satisfied (e.g. state-dependent uncertainty), instability cannot be ruled out (cf. [24], [25]): in the attitude dynamics of a quadrotor, state-dependent uncertainty naturally occurs owing to the Coriolis terms. Crucially, the adaptive control solutions [13], [15]–[17] rely on ‘collocated design’ of underactuated systems [25], i.e. these methods only track the actuated coordinates (altitude, roll, pitch and yaw) considering the non-actuated coordinates (lateral (x, y) position) to be stable a priori. However, external disturbances in lateral position may compromise system stability (cf. [25]).

In view of the above discussions and to the best of the knowledge of the authors, an adaptive control solution for quadrotor is still missing in the presence of *completely unknown state-dependent uncertainty and external disturbances*. Toward this direction, the proposed adaptive solution has the following major contributions:

- An adaptive controller for quadrotor is formulated, which does not require any a priori knowledge of the system dynamic parameters, payload and of disturbances.
- Differently from [13]–[17], the control framework considers six degrees-of-freedom (DoF) dynamics with unknown external perturbations affecting both actuated and non-actuated sub-dynamics.
- The closed-loop stability of the system is analysed via Lyapunov-based method and comparative simulation results suggest significant improvement in tracking accuracy compared to the state of the art.

Note that compared to our previous work [24] dealing with fully actuated systems, the present one is developed for underactuated quadrotor system; further, compared to [25]

dealing with a class of underactuated systems, the present work does not require any knowledge of mass/inertia matrix.

The rest of the paper is organised as follows: Sect. II describes the quadrotor dynamics and the control problem; Sects. III and IV detail the proposed control framework and its stability analysis respectively; Sect. V provides comparative simulation results while Sect. VI provides concluding remarks.

The following notations are used in this paper: $\text{sgn}(s) = [\text{sgn}(s_1), \dots, \text{sgn}(s_n)]$ for $s = [s_1, \dots, s_n]$; $\|\cdot\|$ and $\lambda_{\min}(\cdot)$ denote 1-norm and minimum eigenvalue of (\cdot) , respectively; I denotes identity matrix with appropriate dimension and $\text{diag}\{\cdot, \dots, \cdot\}$ denotes a diagonal matrix.

II. QUADROTOR SYSTEM DYNAMICS AND PROBLEM FORMULATION

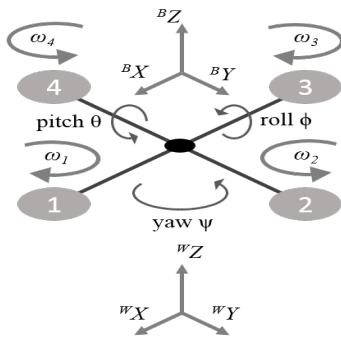


Fig. 1. Schematic of quadrotor with coordinate frames

Let us consider the Euler-Lagrange system dynamics of a quadrotor model (cf. Fig. 1), widely used in literature ([14])

$$m\ddot{p} + G + d_p = \tau_p, \quad (1)$$

$$J(q)\ddot{q} + C_q(q, \dot{q})\dot{q} + d_q = \tau_q, \quad (2)$$

$$\tau_p = R_B^W U, \quad (3)$$

where (1) and (2) are the position and attitude dynamics of the quadrotor, respectively. Various symbols in the dynamics (1) and (2) are described as follows: $m \in \mathbb{R}^+$ and $J(q) \in \mathbb{R}^{3 \times 3}$ represent the mass and inertia matrix, respectively; $p(t) \triangleq [x(t) \ y(t) \ z(t)]^T \in \mathbb{R}^3$ is the position vector of the center of mass of the quadrotor; $q(t) \triangleq [\phi(t) \ \theta(t) \ \psi(t)]^T \in \mathbb{R}^3$ is the orientation/attitude (roll, pitch, yaw angles respectively); $G \triangleq [0 \ 0 \ mg]^T \in \mathbb{R}^3$ is the gravitational force; $C_q(q, \dot{q}) \in \mathbb{R}^{3 \times 3}$ is the Coriolis matrix; $d_p(t)$ and $d_q(t)$ denote the unknown disturbances in position and attitude dynamics, respectively; $\tau_q \triangleq [u_2(t) \ u_3(t) \ u_4(t)]^T \in \mathbb{R}^3$ are the control inputs for roll, pitch and yaw; $\tau_p(t) \in \mathbb{R}^3$ is the generalized control input for position tracking in Earth-fixed frame, with $U(t) \triangleq [0 \ 0 \ u_1(t)]^T \in \mathbb{R}^3$ being the force vector in body-fixed frame and $R_B^W \in \mathbb{R}^{3 \times 3}$ being the Z–Y–X Euler angle rotation matrix describing the rotation from the body-fixed to the Earth-fixed frame, given by

$$R_B^W = \begin{bmatrix} c_\psi c_\theta & c_\psi s_\theta s_\phi - s_\psi c_\phi & c_\psi s_\theta c_\phi + s_\psi s_\phi \\ s_\psi c_\theta & s_\psi s_\theta s_\phi + c_\psi c_\phi & s_\psi s_\theta c_\phi - c_\psi s_\phi \\ -s_\theta & s_\phi c_\theta & c_\theta c_\phi \end{bmatrix}, \quad (4)$$

where $c_{(\cdot)}, s_{(\cdot)}$ and denote $\cos(\cdot), \sin(\cdot)$ respectively.

As per the Euler-Lagrange dynamics, the attitude dynamics of quadrotor satisfy the following properties [14]:

Property 1. The inertia matrix $J(q)$ is uniformly positive definite $\forall q$ and $\exists \underline{j}, \bar{j} \in \mathbb{R}^+$ such that $0 \leq \underline{j}I \leq J(q) \leq \bar{j}I$.

Property 2. $\exists \bar{c}_q, \bar{d}_p, \bar{d}_q \in \mathbb{R}^+$ such that $\|C_q(q, \dot{q})\| \leq \bar{c}_q \|\dot{q}\|$, $\|d_q\| \leq \bar{d}_q$, $\|d_p\| \leq \bar{d}_p$.

Property 3. The matrix $(J - 2C_q)$ is skew symmetric, i.e., for any non-zero vector r , we have $r^T (J - 2C_q) r = 0$.

The following assumption highlights the available knowledge of various system parameters for control design:

Assumption 1: The system dynamics terms m, J, C_q, d_p, d_q and their bounds $\bar{c}_q, \bar{d}_p, \bar{d}_q$ are unknown for control design.

Remark 1 (Knowledge of system dynamics): Assumption 1 is indeed a design challenge: the objective is to formulate a control framework without any knowledge of system parametric uncertainties and external disturbances. Assumption 1 overcomes the need for either precise knowledge of mass/inertia matrix (cf. [9]–[12]), or a priori knowledge of system structures and of bounds on external disturbances (cf. [7], [13]–[16], [18]–[20]).

Remark 2 (Position and attitude tracking co-design):

Tracking control problem of quadrotors can be broadly classified under two categories: (i) reduced-order model based design (cf. [13], [15]–[17]) and (ii) position and attitude tracking co-design (cf. [14], [26]). Control designs relying on the first category ignore the non-actuated (x, y) dynamics and define the control problem as tracking of only the actuated degrees-of-freedom (DoF) i.e. of z and (ϕ, θ, ψ) . Such approach is generally termed as ‘collocated design’ in the literature of underactuated systems (cf. [25]). The second category relies on co-designing position and attitude tracking controller for the six DoF dynamics (1)–(2).

In this work, we shall follow the co-design approach as the reduced-order based approach is conservative for relying on a priori boundedness of (x, y) dynamics. Therefore, we take the following standard assumption:

Assumption 2 ([6], [14], [26]): Let $p_d(t) \triangleq [x_d(t) \ y_d(t) \ z_d(t)]^T$ and $\psi_d(t)$ be the desired position and yaw trajectories to be tracked, which are designed to be sufficiently smooth and bounded.

Remark 3 (Desired roll and pitch): In position and attitude tracking co-design, the desired roll (ϕ_d) and pitch (θ_d) trajectories are derived based on the computed position control input τ_p and the desired yaw trajectory ψ_d (cf. [26]) and it is discussed later (cf. Sect. III.B).

Control Problem: Under Properties 1–3, to design an adaptive controller to track a desired trajectory (cf. Assumption 2) without any knowledge of system dynamics parameters (cf. Assumption 1).

The following section provides a solution to this control problem.

III. CONTROLLER CO-DESIGN

The position and attitude tracking co-design approach consists of simultaneous design of an outer loop controller for position dynamics (1) and of an inner loop controller for

attitude dynamics (2). Following this approach, the proposed control solution is elaborated in the following subsections.

A. Outer Loop Controller

Let us define the position tracking error as $e_p \triangleq p - p_d$ and a sliding variable as

$$s_p = \dot{e}_p + \Phi_p e_p \quad (5)$$

where Φ_p is a positive definite gain matrix. Multiplying the time derivative of (5) by m and using (1) yields

$$m\dot{s}_p = m(\ddot{p} - \ddot{p}_d + \Phi_p \dot{e}_p) = \tau_p + \varphi_p - G \quad (6)$$

where $\varphi_p \triangleq -(d_p + m\ddot{p}_d - m\Phi_p \dot{e}_p)$. Using Property 2, we have

$$\|\varphi_p\| \leq \bar{d}_p + m(\|\ddot{p}_d\| + \|\Phi_p\| \|\dot{e}_p\|). \quad (7)$$

Further, let us define $\xi_p \triangleq [e_p^T \ \dot{e}_p^T]^T$. Then using the inequality $\|\xi_p\| \geq \|\dot{e}_p\|$ and boundedness of the desired trajectories, we have

$$\|\varphi_p\| \leq K_{p0}^* + K_{p1}^* \|\xi_p\| \quad (8)$$

where $K_{p0}^* \triangleq \bar{d}_p + m\|\ddot{p}_d\|$, $K_{p1}^* \triangleq m\|\Phi_p\|$ are *unknown* finite scalars. The outer loop control law is designed as

$$\tau_p(t) = -\Lambda_p s_p(t) - \rho_p(t) \operatorname{sgn}(s_p(t)) + \hat{m}(t) g_p \quad (9a)$$

$$\rho_p(t) = \hat{K}_{p0}(t) + \hat{K}_{p1}(t) \|\xi_p\| \quad (9b)$$

where Λ_p is a positive definite user-defined gain matrix; $g_p = [0 \ 0 \ g]^T$ is the gravity vector; \hat{K}_{pi} and \hat{m} are the estimates of K_{pi}^* and m , $i = 0, 1$ respectively and they are evaluated via the following adaptive laws

$$\dot{\hat{K}}_{pi}(t) = \|s_p(t)\| \|\xi_p(t)\|^i - \alpha_{pi} \hat{K}_{pi}(t), \quad \hat{K}_{pi}(0) > 0 \quad (10a)$$

$$\dot{\hat{m}}(t) = -s_p(t)^T g_p - \alpha_m \hat{m}(t), \quad \hat{m}(0) > 0 \quad (10b)$$

where $\alpha_{pi}, \alpha_m \in \mathbb{R}^+$ are user-defined design scalars. Note that eventually U is applied to the system by transforming τ_p via the relation (3) (R_B^W is invertible rotational matrix), giving non-zero input only in z direction.

B. Inner Loop Controller

To realize the inner loop controller, it is important to generate the desired roll (ϕ_d) and pitch (θ_d) angles. This process involves defining an intermediate coordinate frame as the first step (cf. [26]):

$$z_B = \frac{\tau_p}{\|\tau_p\|} \quad (11a)$$

$$y_A = [-s_{\psi_d} \ c_{\psi_d} \ 0]^T \quad (11b)$$

$$x_B = \frac{y_A \times z_B}{\|y_A \times z_B\|} \quad (11c)$$

$$y_B = z_B \times x_B \quad (11d)$$

where y_A is the y -axis of the intermediate coordinate frame A , x_B , y_B and z_B are the x -axis, y -axis and z -axis of the body fixed coordinate frame. Given the desired yaw angle $\psi_d(t)$ and based on the computed intermediate axes as in (11),

$\phi_d(t)$ and $\theta_d(t)$ can be determined using the desired body frame axes as described in [26].

Further, to achieve the attitude tracking control objective, the error in orientation/attitude is defined as [26]

$$e_q = ((R_d)^T R_B^W - (R_B^W)^T R_d)^v \quad (12)$$

$$\dot{e}_q = \dot{q} - R_d^T R_B^W \dot{q}_d \quad (13)$$

where $(\cdot)^v$ represents *vee* map, which converts elements of $SO(3)$ to $\in \mathbb{R}^3$ [26] and R_d is the rotation matrix as in (4) evaluated at $(\phi_d, \theta_d, \psi_d)$.

The sliding variable s_q for inner loop control is defined as

$$s_q = \dot{e}_q + \Phi_q e_q \quad (14)$$

where Φ_q is a positive definite gain matrix. Multiplying the derivative of (14) by J and using (2) yield

$$J\dot{s}_q = J(\ddot{q} - \ddot{q}_d + \Phi_q \dot{e}_q) = \tau_q - C_q s_q + \varphi_q \quad (15)$$

where $\varphi_q \triangleq -(C_q \dot{q} + d_q + J\ddot{q}_d - J\Phi_q \dot{e}_q - C_q s_q)$ represents the overall uncertainties in attitude dynamics. Using (28) and Properties 1 and 2 we have

$$\|\varphi_q\| \leq \bar{c}_q \|\dot{q}\|^2 + \bar{d}_q + \bar{j}(\|\ddot{q}_d\| + \|\Phi_q\| \|\dot{e}_q\|) + \bar{c}_q \|\dot{q}\|(\|\dot{e}_q\| + \|\Phi_q\| \|\dot{q}\|) \quad (16)$$

Further, let us define $\xi_q \triangleq [e_q^T \ \dot{e}_q^T]^T$. Then using the inequalities $\|\xi_q\| \geq \|e_q\|$, $\|\xi_q\| \geq \|\dot{e}_q\|$, boundedness of the desired trajectories, and substituting $\dot{q} = \dot{e}_q + \dot{q}_d$ in (16) yield

$$\|\varphi_q\| \leq K_{q0}^* + K_{q1}^* \|\xi_q\| + K_{q2}^* \|\xi_q\|^2, \quad (17)$$

where $K_{q0}^* \triangleq \bar{c}_q \|\dot{q}_d\|^2 + \bar{d}_q + \bar{j} \|\ddot{q}_d\|$, $K_{q1}^* \triangleq \bar{c}_q \|\dot{q}_d\| (3 + \|\Phi_q\|) + \bar{j} \|\Phi_q\|$, $K_{q2}^* \triangleq \bar{c}_q \|\dot{q}_d\| (2 + \|\Phi_q\|)$ are *unknown* finite scalars.

The inner loop control law is designed as

$$\tau_q(t) = -\Lambda_q s_q(t) - \rho_q(t) \operatorname{sgn}(s_q(t)), \quad (18a)$$

$$\rho_q(t) = \hat{K}_{q0}(t) + \hat{K}_{q1}(t) \|\xi_q(t)\| + \hat{K}_{q2}(t) \|\xi_q(t)\|^2, \quad (18b)$$

where Λ_q is a positive definite user-defined gain matrix and \hat{K}_{qi} , $i = 0, 1, 2$ are the estimates of K_{qi}^* adapted via the following law:

$$\dot{\hat{K}}_{qi}(t) = \|s_q(t)\| \|\xi_q(t)\|^i - \alpha_{qi} \hat{K}_{qi}(t), \quad \hat{K}_{qi}(0) > 0, \quad (19)$$

where $\alpha_{qi} \in \mathbb{R}^+$, $i = 0, 1, 2$ are user-defined scalars.

Remark 4 (On state-dependent uncertainty): The inequalities (8) and (17) reveal that state-dependencies occur inherently in the upper bound structures of uncertainties via ξ_p and ξ_q . Therefore, conventional adaptive sliding mode designs such as [17], [21]–[23] are not feasible as state-dependent uncertainty cannot be bounded a priori. On the other hand, the gains ρ_p in (9b) and ρ_q in (18b) are designed according to the state-dependent uncertainty structures (8) and (17) respectively.

Remark 5 (On co-design of outer and inner loop): Note that the inner and outer loop design processes are coupled via τ_p and simultaneously affect the quadrotor system: this makes the proposed design a more realistic one compared to decoupled dynamics based approaches (cf. [13], [15]–[17]) or linearized and decoupled autopilot based designs (cf. [27], [28]).

IV. STABILITY ANALYSIS OF THE PROPOSED CONTROLLER

Theorem 1: Under Properties 1-3 and Assumptions 1-2, the trajectories of the closed-loop systems (6) and (15) using the control laws (9) and (18) along with the adaptive laws (10) and (19) are Uniformly Ultimately Bounded (UUB).

Proof: Note that the solutions of the adaptive gains (10a) and (19) yield $\hat{K}_{pi}(t) \geq 0$, $i = 0, 1$ and $\hat{K}_{qi}(t) \geq 0$, $i = 0, 1, 2 \forall t \geq 0$ (cf. [24] for details).

Closed-loop stability is analysed using the following Lyapunov function

$$V = V_p + V_q, \quad (20)$$

$$\text{where } V_p = \frac{1}{2} s_p^T m s_p + \frac{1}{2} \sum_{i=0}^1 (\hat{K}_{pi} - K_{pi}^*)^2 + \frac{1}{2} (\hat{m} - m)^2 \quad (21)$$

$$V_q = \frac{1}{2} s_q^T J s_q + \frac{1}{2} \sum_{i=0}^2 (\hat{K}_{qi} - K_{qi}^*)^2. \quad (22)$$

Using (6) and (15), the time derivatives of (21) and (22) yield

$$\begin{aligned} \dot{V}_p &= s_p^T m \dot{s}_p + \sum_{i=0}^1 (\hat{K}_{pi} - K_{pi}^*) \dot{\hat{K}}_{pi} + (\hat{m} - m) \dot{\hat{m}} \\ &= s_p^T (\tau_p + \varphi_p + G) + \sum_{i=0}^1 (\hat{K}_{pi} - K_{pi}^*) \dot{\hat{K}}_{pi} + (\hat{m} - m) \dot{\hat{m}} \quad (23) \end{aligned}$$

$$\begin{aligned} \dot{V}_q &= s_q^T J \dot{s}_q + \frac{1}{2} s_q^T \dot{J} s_q + \sum_{i=0}^2 (\hat{K}_{qi} - K_{qi}^*) \dot{\hat{K}}_{qi} \\ &= s_q^T (\tau_q - C_q s_q + \varphi_q) + \frac{1}{2} s_q^T \dot{J} s_q + \sum_{i=0}^2 (\hat{K}_{qi} - K_{qi}^*) \dot{\hat{K}}_{qi} \quad (24) \end{aligned}$$

Utilizing the upper bound structure given by (8) and Property 2, and the control laws (9), (18), the terms \dot{V}_p in (23) and \dot{V}_q in (24) are simplified to

$$\begin{aligned} \dot{V}_p &= s_p^T (-\Lambda_p s_p - \rho_p \text{sgn}(s_p) + \hat{m} g_p + \varphi_p - G) \\ &\quad + \sum_{i=0}^1 (\hat{K}_{pi} - K_{pi}^*) \dot{\hat{K}}_{pi} + (\hat{m} - m) \dot{\hat{m}} \quad (25) \end{aligned}$$

$$\begin{aligned} \dot{V}_q &= s_q^T (-\Lambda_q s_q - \rho_q \text{sgn}(s_q) + \varphi_q) \\ &\quad + \frac{1}{2} s_q^T (\dot{J} - 2C_q) s_q + \sum_{i=0}^2 (\hat{K}_{qi} - K_{qi}^*) \dot{\hat{K}}_{qi} \quad (26) \end{aligned}$$

Property 3 implies that $s_q^T (J - 2C_q) s_q = 0$. Then utilizing the upper bound structure (8) and (17), and the facts that $G = m g_p$, $\rho_p \geq 0$, $\rho_q \geq 0$ we have

$$\begin{aligned} \dot{V}_p &= -s_p^T \Lambda_p s_p - \sum_{i=0}^1 (\hat{K}_{pi} - K_{pi}^*) (|\xi_p|^i \|s_p\| - \dot{\hat{K}}_{pi}) \\ &\quad + (\hat{m} - m) (s_p^T g_p + \dot{\hat{m}}) \quad (27) \end{aligned}$$

$$\dot{V}_q = -s_q^T \Lambda_q s_q - \sum_{i=0}^2 (\hat{K}_{qi} - K_{qi}^*) (|\xi_q|^i \|s_q\| - \dot{\hat{K}}_{qi}) \quad (28)$$

Using (10) and (19), we have

$$(\hat{K}_{pi} - K_{pi}^*) \dot{\hat{K}}_{pi} = \|s_p\| (\hat{K}_{pi} - K_{pi}^*) |\xi_p|^i + \alpha_{pi} \hat{K}_{pi} K_{pi}^* - \alpha_{pi} \hat{K}_{pi}^2 \quad (29)$$

$$(\hat{m} - m) \dot{\hat{m}} = -(\hat{m} - m) s_p^T g_p + \alpha_m \hat{m} m - \alpha_m \hat{m}^2 \quad (30)$$

$$(\hat{K}_{qi} - K_{qi}^*) \dot{\hat{K}}_{qi} = \|s_q\| (\hat{K}_{qi} - K_{qi}^*) |\xi_q|^i + \alpha_{qi} \hat{K}_{qi} K_{qi}^* - \alpha_{qi} \hat{K}_{qi}^2 \quad (31)$$

Substituting (29)-(31) into (27) and (28) yield

$$\begin{aligned} \dot{V}_p &\leq -\frac{\lambda_{\min}(\Lambda_p) \|s_p\|^2}{3} + \sum_{i=0}^1 (\alpha_{pi} \hat{K}_{pi} K_{pi}^* - \alpha_{pi} \hat{K}_{pi}^2) \\ &\quad + \alpha_m \hat{m} m - \alpha_m \hat{m}^2 \\ &\leq -\frac{\lambda_{\min}(\Lambda_p) \|s_p\|^2}{3} - \sum_{i=0}^2 \frac{\alpha_{pi}}{2} \left((\hat{K}_{pi} - K_{pi}^*)^2 - K_{pi}^{*2} \right) \\ &\quad - (\alpha_m/2) (\hat{m} - m)^2 + (\alpha_m/2) m^2 \quad (32) \end{aligned}$$

$$\begin{aligned} \dot{V}_q &\leq -\frac{\lambda_{\min}(\Lambda_q) \|s_q\|^2}{3} + \sum_{i=0}^2 (\alpha_{qi} \hat{K}_{qi} K_{qi}^* - \alpha_{qi} \hat{K}_{qi}^2) \\ &\leq -\frac{\lambda_{\min}(\Lambda_q) \|s_q\|^2}{3} - \sum_{i=0}^2 \frac{\alpha_{qi}}{2} \left((\hat{K}_{qi} - K_{qi}^*)^2 - K_{qi}^{*2} \right) \quad (33) \end{aligned}$$

Further the definition of Lyapunov function yields

$$V_p \leq \frac{m}{2} \|s_p\|^2 + \frac{1}{2} \sum_{i=0}^1 (\hat{K}_{pi} - K_{pi}^*)^2 + \frac{1}{2} (\hat{m} - m)^2 \quad (34)$$

$$V_q \leq \frac{\bar{J}}{2} \|s_q\|^2 + \frac{1}{2} \sum_{i=0}^2 (\hat{K}_{qi} - K_{qi}^*)^2. \quad (35)$$

From (34) and (35), the conditions (32) and (33) can be further simplified to

$$\dot{V}_p \leq -\varrho_p V_p + \frac{1}{2} \sum_{i=0}^1 \alpha_{pi} K_{pi}^{*2} + \frac{1}{2} \alpha_m m^2 \quad (36)$$

$$\dot{V}_q \leq -\varrho_q V_q + \frac{1}{2} \sum_{i=0}^2 \alpha_{qi} K_{qi}^{*2} \quad (37)$$

where $\varrho_p \triangleq \frac{\min_i \{\lambda_{\min}(\Lambda_p)/3, \alpha_{pi}, \alpha_m\}}{\max\{m/2, 1/2\}}$, $\varrho_q \triangleq \frac{\min_i \{\lambda_{\min}(\Lambda_q)/3, \alpha_{qi}\}}{\max\{\bar{J}/2, 1/2\}} > 0$ can be designed via (9a), (10), (18a), and (19). From (36) and (37), the upper bound for the time derivative of the overall Lyapunov function \dot{V} can be obtained as

$$\dot{V} \leq -\varrho V + \frac{1}{2} \sum_{i=0}^1 (\alpha_{pi} K_{pi}^{*2} + \alpha_{qi} K_{qi}^{*2}) + \frac{1}{2} \alpha_m m^2. \quad (38)$$

where $\varrho = \min\{\varrho_p, \varrho_q\}$. Defining a scalar κ such that $0 < \kappa < \varrho$, (38) is simplified to

$$\dot{V} = -\kappa V - (\varrho - \kappa) V + \frac{1}{2} \sum_{i=0}^1 (\alpha_{pi} K_{pi}^{*2} + \alpha_{qi} K_{qi}^{*2} + \alpha_m m^2). \quad (39)$$

Defining a scalar $\bar{\mathcal{B}} \triangleq \frac{(\sum_{i=0}^1 \alpha_{pi} K_{pi}^{*2} + \alpha_{qi} K_{qi}^{*2}) + \alpha_m m^2}{2(\varrho - \kappa)}$, it can be seen that $\dot{V}(t) < -\kappa V(t)$ when $V(t) \geq \bar{\mathcal{B}}$, so that

$$V \leq \max\{V(0), \bar{\mathcal{B}}\}, \forall t \geq 0, \quad (40)$$

and the closed-loop system remains UUB (cf. UUB definition 4.6 as in [29]). ■

Remark 6: Control laws (9a) and (18a) are discontinuous in nature, which may cause chattering. Therefore, as standard

for sliding mode designs, the control laws can be made continuous by replacing the ‘signum’ function by a ‘saturation’ function defined as $\text{sat}(s_p, \bar{\omega}_p) = s_p / \|s_p\|$ (resp. $s_p / \bar{\omega}_p$) if $\|s_p\| \geq \bar{\omega}_p$ (resp. $\|s_p\| < \bar{\omega}_p$) where $\bar{\omega}_p \in \mathbb{R}^+$ is a small scalar used to avoid chattering. Similarly, $\text{sgn}(s_q)$ can be modified. Such modifications do not change the closed-loop stability result albeit some minor modifications in stability analysis, which can be carried out in the same line as in [30].

V. SIMULATION RESULTS AND ANALYSIS

The performance of the proposed controller is tested on a Gazebo simulation platform using the RotorS Simulator framework [31] for ROS with the Pelican quadrotor model. The results of the proposed adaptive sliding mode controller (ASMC) is compared with the geometric controller [32] (referred as PD control hereafter) available in the RotorS framework and sliding mode controller (SMC) [9]. The Gazebo model of quadrotor can be actuated by commanding the angular velocities for the rotors following the relationship between thrust, moments and angular velocities as in [26]:

1) *Simulation Scenario and Parameter Selection:* To properly judge the performance of the proposed design, an aggressive manoeuvring scenario is created. To this end, a set of way-points (x_d, y_d, z_d) and ψ_d are commanded as input to the controllers (cf. Fig. 2). These abrupt transitions between the positions demand aggressive manoeuvres for a fast response. For time duration $0 \leq t < 48\text{s}$, the set of way-points are commanded without any payload attached to the quadrotor. Then, at $t = 48\text{s}$, a payload of 0.5 kg is added to the quadrotor (the system weighs 2 kg without any payload) and the same set of way-points are repeated.

For simulation, the control parameters of the proposed ASMC are selected to be: $\Phi_p = \text{diag}\{2.4, 2.4, 16\}$, $\Phi_q = \text{diag}\{0.22, 0.22, 0.01\}$, $\Lambda_p = \text{diag}\{1.2, 1.2, 0.8\}$, $\Lambda_q = \text{diag}\{4.5, 4.5, 3.5\}$, $\hat{K}_{p0}(0) = \hat{K}_{p1}(0) = 0.01$, $\hat{K}_{q0}(0) = \hat{K}_{q1}(0) = \hat{K}_{q2}(0) = 0.0001$, $\alpha_{p0} = \alpha_{p1} = 3$, $\alpha_{q0} = \alpha_{q1} = \alpha_{q2} = 50$, $\hat{m}(0) = 0.01$ and $\alpha_m = 0.1$, $\bar{\omega}_p = 0.1$, $\bar{\omega}_q = 1$. For a fair comparison, similar sliding surfaces are selected for SMC as in (5) and (14). The gains for PD controller [32] is selected to be same as in the RotorS package, which are optimized for the Pelican model. Initial position and attitude for the quadrotor are selected to be $x(0) = y(0) = 0$, $z(0) = 0.1$ and $\phi(0) = \theta(0) = \psi(0) = 0$.

2) *Results and Analysis:* Figures 2-4 depict the position tracking with various controllers and the corresponding errors incurred by them in position and attitude. It can be noted at $t \geq 72\text{s}$, the altitude (z position) of the quadrotor using PD controller has become zero, i.e., the quadrotor has crashed on the floor during the manoeuvres after adding the payload. Reduction in the z position error for the PD controller at $t > 82\text{s}$ should not be confused to be performance improvement: it is a result of reduction in the desired altitude z_d (cf. Fig. 2), whereas the quadrotor still remains crashed on the ground.

For better inference, a performance comparison via root-mean-squared (RMS) error between SMC and ASMC is provided in Table I after payload is attached, i.e., for $t \geq 48\text{s}$ (since the quadrotor crashed during the scenario for

TABLE I
PERFORMANCE COMPARISON

| position | RMS error (m) | | | RMS error (degree) | | |
|-----------------|---------------|------|------|--------------------|----------|--------|
| | x | y | z | ϕ | θ | ψ |
| SMC | 0.47 | 0.69 | 0.65 | 3.70 | 4.06 | 9.90 |
| ASMC (proposed) | 0.40 | 0.48 | 0.42 | 3.80 | 2.67 | 10.06 |

geometric controller, its RMS error data is not tabulated). It clearly demonstrates the superior position tracking performance of the proposed scheme, where it has delivered a minimum performance improvement of 14.5%. Despite position tracking is of more importance for transportation, it is also worth mentioning that attitude tracking of both the controllers are, however, almost similar. This is caused by the higher transients for ASMC compared to SMC, during the sharp changes in desired trajectory. This happens because the gains of ASMC need to re-adapt itself every time with the sharp changes in trajectories, while gains for SMC are fixed and less sensitive to abrupt changes. These transients are inherent for any adaptive design, but it helps them to adjust with unknown changes while fixed-gain designs can fail when uncertainties lie beyond the a priori knowledge.

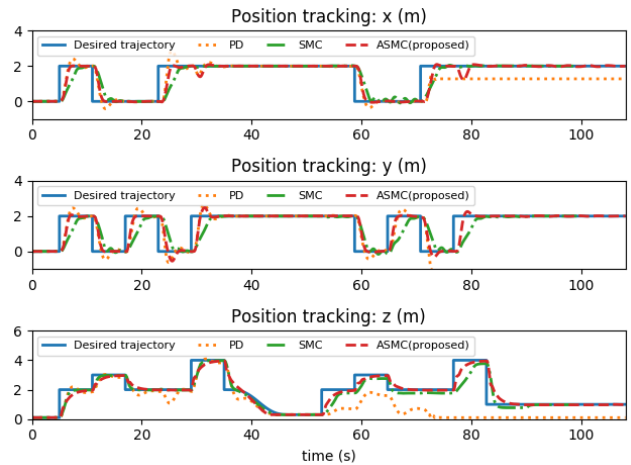


Fig. 2. Position tracking comparison for aggressive manoeuvre

VI. CONCLUSION

An adaptive controller for quadrotors was proposed, which can tackle parametric uncertainties and external disturbances without their a priori knowledge and can negotiate possibly a priori unbounded state-dependent uncertainties. Closed-loop system stability was established via the notion of uniformly ultimately boundedness. The effectiveness of the proposed controller was comparatively verified against state-of-the-art methods under various scenarios using Gazebo simulation using RotorS Simulator framework.

REFERENCES

- [1] L. Fusini, T. I. Fossen, and T. A. Johansen, “Nonlinear observers for GNSS- and camera-aided inertial navigation of a fixed-wing UAV,” *IEEE Transactions on Control Systems Technology*, vol. 26, no. 5, pp. 1884–1891, 2018.

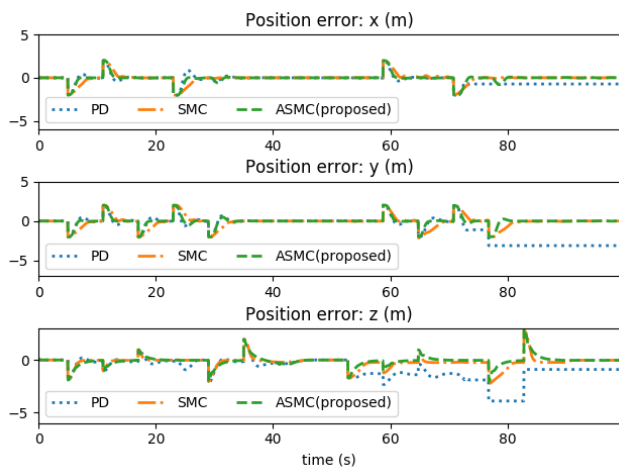


Fig. 3. Position tracking error comparison for aggressive manoeuvre

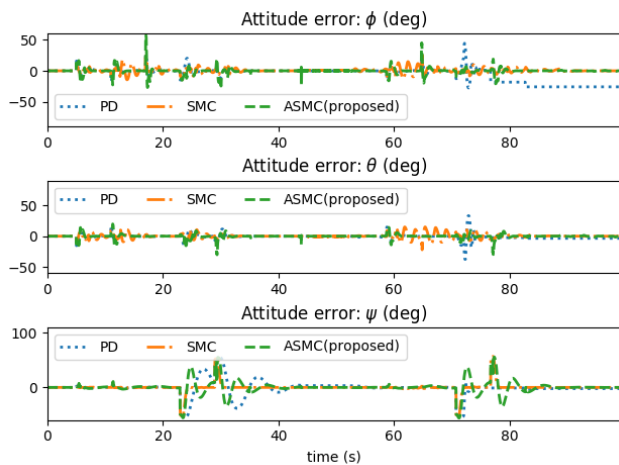


Fig. 4. Attitude tracking error comparison for aggressive manoeuvre

[2] A. C. Kapoutsis, S. A. Chatzichristofis, L. Doitsidis, J. B. de Sousa, and E. B. Kosmatopoulos, "Autonomous navigation of teams of unmanned aerial or underwater vehicles for exploration of unknown static & dynamic environments," in *21st Mediterranean Conference on Control and Automation*. IEEE, 2013, pp. 1181–1188.

[3] Y. Y. Nazaruddin, A. Widyotriatmo, T. A. Tamba, M. S. Arifin, and R. A. Santosa, "Communication-efficient optimal-based control of a quadrotor UAV by event-triggered mechanism," in *2018 5th Asian Conference on Defense Technology (ACDT)*. IEEE, 2018, pp. 96–101.

[4] D. Invernizzi, M. Lovera, and L. Zaccarian, "Dynamic attitude planning for trajectory tracking in thrust-vectoring UAVs," *IEEE Transactions on Automatic Control*, vol. 65, no. 1, pp. 453–460, 2019.

[5] —, "Integral ISS-based cascade stabilization for vectored-thrust UAVs," *IEEE Control Systems Letters*, vol. 4, no. 1, pp. 43–48, 2019.

[6] S. Tang and V. Kumar, "Mixed integer quadratic program trajectory generation for a quadrotor with a cable-suspended payload," *IEEE International Conference on Robotics and Automation (ICRA)*, pp. 2216–2222, 2015.

[7] S. Yang and B. Xian, "Energy-based nonlinear adaptive control design for the quadrotor UAV system with a suspended payload," *IEEE Transactions on Industrial Electronics*, vol. 67, no. 3, pp. 2054–2064, 2019.

[8] K. Sreenath, N. Michael, and V. Kumar, "Trajectory generation and control of a quadrotor with a cable-suspended load—a differentially-flat hybrid system," in *2013 IEEE International Conference on Robotics and Automation*. IEEE, 2013, pp. 4888–4895.

[9] R. Xu and Ü. Özgüner, "Sliding mode control of a class of underactuated systems," *Automatica*, vol. 44, no. 1, pp. 233–241, 2008.

[10] A. Sanchez, V. Parra-Vega, C. Tang, F. Oliva-Palomo, and C. Izaguirre-Espinosa, "Continuous reactive-based position-attitude control of quadrotors," in *2012 American Control Conference (ACC)*. IEEE, 2012, pp. 4643–4648.

[11] L. Derafa, A. Benallegue, and L. Fridman, "Super twisting control algorithm for the attitude tracking of a four rotors UAV," *Journal of the Franklin Institute*, vol. 349, no. 2, pp. 685–699, 2012.

[12] T. Madani and A. Benallegue, "Sliding mode observer and backstepping control for a quadrotor unmanned aerial vehicles," in *2007 American Control Conference*. IEEE, 2007, pp. 5887–5892.

[13] C. Nicol, C. Macnab, and A. Ramirez-Serrano, "Robust adaptive control of a quadrotor helicopter," *Mechatronics*, vol. 21, no. 6, pp. 927–938, 2011.

[14] B. J. Bialy, J. Klotz, K. Brink, and W. E. Dixon, "Lyapunov-based robust adaptive control of a quadrotor UAV in the presence of modeling uncertainties," *American Control Conference*, pp. 13–18, 2013.

[15] Z. T. Dydek, A. M. Annaswamy, and E. Lavretsky, "Adaptive control of quadrotor UAVs: A design trade study with flight evaluations," *IEEE Transactions on Control Systems Technology*, vol. 21, no. 4, pp. 1400–1406, 2012.

[16] C. Ha, Z. Zuo, F. B. Choi, and D. Lee, "Passivity-based adaptive backstepping control of quadrotor-type UAVs," *Robotics and Autonomous Systems*, vol. 62, no. 9, pp. 1305–1315, 2014.

[17] O. Mofid and S. Mobayen, "Adaptive sliding mode control for finite-time stability of quad-rotor UAVs with parametric uncertainties," *ISA Transactions*, vol. 72, pp. 1–14, 2018.

[18] T.-T. Tran, S. S. Ge, and W. He, "Adaptive control of a quadrotor aerial vehicle with input constraints and uncertain parameters," *International Journal of Control*, vol. 91, no. 5, pp. 1140–1160, 2018.

[19] B. Tian, J. Cui, H. Lu, Z. Zuo, and Q. Zong, "Adaptive finite-time attitude tracking of quadrotors with experiments and comparisons," *IEEE Transactions on Industrial Electronics*, 2019.

[20] B. Zhao, B. Xian, Y. Zhang, and X. Zhang, "Nonlinear robust adaptive tracking control of a quadrotor UAV via immersion and invariance methodology," *IEEE Transactions on Industrial Electronics*, vol. 62, no. 5, pp. 2891–2902, 2014.

[21] Y. Shtessel, M. Taleb, and F. Plestan, "A novel adaptive-gain super-twisting sliding mode controller: Methodology and application," *Automatica*, vol. 48, no. 5, pp. 759–769, 2012.

[22] V. I. Utkin and A. S. Poznyak, "Adaptive sliding mode control with application to super-twist algorithm: Equivalent control method," *Automatica*, vol. 49, no. 1, pp. 39–47, 2013.

[23] H. Obeid, L. M. Fridman, S. Laghrouche, and M. Harmouche, "Barrier function-based adaptive sliding mode control," *Automatica*, vol. 93, pp. 540–544, 2018.

[24] S. Roy, S. Baldi, and L. M. Fridman, "On adaptive sliding mode control without a priori bounded uncertainty," *Automatica*, vol. 111, p. 108650, 2020.

[25] S. Roy and S. Baldi, "Towards structure-independent stabilization for uncertain underactuated Euler–Lagrange systems," *Automatica*, vol. 113, p. 108775, 2020.

[26] D. Mellinger and V. Kumar, "Minimum snap trajectory generation and control for quadrotors," in *2011 IEEE International Conference on Robotics and Automation*. IEEE, 2011, pp. 2520–2525.

[27] S. Fari, X. Wang, S. Roy, and S. Baldi, "Addressing unmodelled path-following dynamics via adaptive vector field: A UAV test case," *IEEE Transactions on Aerospace and Electronic Systems*, 2019.

[28] J. Yang, X. Wang, S. Baldi, S. Singh, and S. Fari, "A software-in-the-loop implementation of adaptive formation control for fixed-wing UAVs," *IEEE/CAA Journal of Automatica Sinica*, vol. 6, no. 5, pp. 1230–1239, 2019.

[29] H. K. Khalil, *Nonlinear systems*. Prentice hall Upper Saddle River, NJ, 2002, vol. 3.

[30] S. Roy, S. B. Roy, J. Lee, and S. Baldi, "Overcoming the underestimation and overestimation problems in adaptive sliding mode control," *IEEE/ASME Transactions on Mechatronics*, vol. 24, no. 5, pp. 2031–2039, 2019.

[31] F. Furrer, M. Burri, M. Achtelik, and R. Siegwart, *RotorS – A Modular Gazebo MAV Simulator Framework*, 01 2016, vol. 625, pp. 595–625.

[32] T. Lee, M. Leok, and N. H. McClamroch, "Geometric tracking control of a quadrotor UAV on SE(3)," in *49th IEEE Conference on Decision and Control (CDC)*. IEEE, 2010, pp. 5420–5425.